Utilization of Near Infrared Fluorescence Imaging to Track and Quantify the Pulmonary Retention of Single-Walled Carbon Nanotubes in Mice

Justine Nicholas[a,b], **Hao Chen**[b], **Keira Liu**[c], **Indu Venu**[e], **Donald Bolser**[b], **Navid B. Saleh**[e], **Joseph H. Bisesi Jr**[a], **William Castleman**[d], **P. Lee Ferguson**[c], **Tara Sabo-Attwood**[a]

[a]Department of Environmental and Global Health, University of Florida, Gainesville, FL 32610, United States;

[b]Department of Physiological Sciences, University of Florida, Gainesville, FL 32610, United States

[c]Department of Civil and Environmental Engineering, Nicholas School of the Environment, Duke University, Durham, NC, 27708, United States;

[d]Department of Infectious Disease and Pathology, University of Florida, Gainesville, FL 32610, United States;

[e]Department of Civil, Architectural and Environmental Engineering, University of Texas, Austin TX, 78712, United States.

Abstract

As nanomaterials are used in a wide array of applications, investigations regarding health impacts associated with inhalation are a concern. Reports show that exposure to single-walled carbon nanotubes (SWCNTs) can induce fibrosis, allergic-type reactions, and pathogen susceptibility. Airway clearance is known to play a primary role in these disease states, yet SWCNT detection in biological systems is challenging. Common techniques, such as electron microscopy, lack spatial resolution and specificity to delineate SWCNTs in carbon-based organisms. Here we validated a near-infrared fluorescence imaging (NIRFI) system to track and semi-quantify SWCNTs over 21 days in tissues of mice exposed intratracheally to 1 dose of SWCNTs. In tandem, we optimized a NIRF-based spectrometry method to quantify SWCNTs, showing that NIRFI was consistent with SWCNT burdens quantified by NIRF spectroscopy in whole lung tissue homogenates. Finally, NIRFI was utilized to localize SWCNTs on lung tissue sections used for pathological analysis. Results revealed that SWCNTs remained in the lung over 21 days and were consistent with

*Corresponding Author:** Tara Sabo-Attwood. Department of Environmental and Global Health, Center for Environmental and Human Toxicology, University of Florida, Box 110885, 2187 Mowry Rd., Gainesville, FL 32611. sabo@phhp.ufl.edu. Phone: (352) 294-5293.

alveolar wall restructuring and granuloma formation. This study is the first to quantify SWCNTs in mouse lungs using both semi-quantitative tracking and quantitative mass measurements using NIRF, highlighting this as a sensitive and specific technique for assessing SWCNT clearance *in vivo*.

Keywords

Carbon nanotubes; lung; detection; near-infrared; mice

1.0. Introduction

Tracking and quantifying carbon-based nanomaterials in biological systems presents unique challenges yet it is imperative to understanding their potential for adverse health effects. It is evident that lack of pulmonary clearance of inhaled particles and fibers can contribute significantly to injury and disease including fibrosis, cancer and mesothelioma[1–2]. Therefore assessing particle clearance *in vivo* has direct relevance to advancing our understanding of their potential to cause long term health effects. Several analytical methods have been commonly employed for carbon nanomaterial (NM) detection including electron microscopy (TEM/SEM), Raman, and inductively coupled plasma mass spectrometry (ICP-MS); but each has limitations that include spatial resolution and lack of specificity for differentiating carbon nanomaterials from the carbon in the biomass of living organisms[3–4]. Near infrared fluorescence-based approaches have emerged as a promising tool for detection and quantification of single-walled carbon nanotubes (SWCNTs) in environmental samples[5–6]. We recently demonstrated that near infrared fluorescence (NIRF) was an effective method for tracking pristine (non-functionalized surface) SWCNTs in fish species; however, no studies to date have utilized such methods for localizing and quantifying SWCNTs in pulmonary tissues[5]. Here we have optimized NIRF imaging (NIRFI) and quantitation methods to examine the pulmonary retention of SWCNTs in a murine model. To accomplish this we utilized a custom NIRFI system that allows for both visualization and semi-quantification of SWCNTs in whole organs and histological tissue sections. We also optimized a spectroscopic method to quantify SWCNTs in lung tissue homogenates. Finally, we employed these methods in a proof of concept study, where mice were exposed with a single dose of SWCNTs by intratracheal instillation (20 μg/mouse), and their pulmonary localization and retention was tracked and quantified using our NIRF methods over a 21 day time period.

2.0. Experimental Section

2.1. SWCNT Preparation

Pristine SWCNTs (SG65i) were provided by SouthWest Nanotechnologies Inc. (Norman, OK). The SG65i are semiconductive (6, 5) chirality-enriched, non-functionalized SWCNTs, measuring 0.78 nm in average diameter (Figure 1) and containing <4% by mass the metal catalysts cobalt and molybdenum. It should be noted that we did not remove metals in house because we wanted to utilize 'as purchased' SWCNTs in the form they are likely to be used in products and applications. Also, removing all metals is not practical without significantly

changing the physicochemical structure and properties of the SWCNTs themselves. Acid-leaching is performed during the manufacturing process to remove 'labile' metals, but even strong acids cannot access all of the metals associated with the SWCNTs. Such processing may therefore change the innate fluorescent properties needed for NIRFI. We quantified metals in a series of leaching studies previously[5, 7] and on suspensions used in the current study and therefore have a good understanding of the minimal amount of metals that separate from SWCNTs in biological systems (*in vitro*). Results of these experiments showed that only 3.8% and 1.001% (w/w) of the total cobalt and molybdenum (< 4%), respectively, leached from a SWCNT suspension (pluronic) into cell media (Figure S1).

SWCNT suspensions were prepared in 2% sodium deoxycholate (SDC) and dialyzed in 1 % pluronic F88 (v/v in deionized water, Sigma) over a three day period using a method reported by Welsher and colleagues with modification[4]. Pluronic is a well-recognized suspension medium for particulates like nanotubes and has been used extensively in *in vitro* and *in vivo* exposures by us and others[8–11]. It is used primarily because it is biocompatible (no observed toxicity) while still allowing CNTs to exist as aggregates that are nano-sized (as shown through extensive characterization[5–7, 9, 12]). For these studies we suspended SWCNTs in SDC and then dialyzed them against a pluronic solutions so they retain the spectral characteristics of the SDC suspended SWCNTs, which is why this dialysis process allows for greater fluorescence intensity over using pluronic suspended SWCNTs without initial suspension in SDC. Based on the photophysical behavior of SWCNTs, we expect that this observation is a result of the nanotubes essentially remaining disaggregated after dialysis, whereas pluronic suspended SWCNTs are less efficiently dispersed.

To prepare suspensions, 1mg/ml dry SWCNTs were suspended in 2% SDC, cooled using an ice bath, and sonicated first at 30% power for 10 mins followed by sonication at a 50% power for an additional 10 minutes (Sonifier™ S-450 Digital Ultrasonic Cell Disruptor/Homogenizer, Branson Ultrasonics, Danbury, CT). A 1:50 dilution of the suspension was prepared using 2% sodium cholate for absorbance measurement read at 775 nm (SOFTmax Pro 4.0)[9]. The remaining suspension was then centrifuged at 14,100 g for 20 minutes. Finally the supernatant was sonicated at 30 % power for 10 minutes and absorbance measurements read once again. The suspension was then evenly placed into a pre-soaked (initially soaked for 2 minutes in 1 % pluronic) 3 ml dialysis cartridges (10000 MWCO, Thermo-Scientific). For optimal surfactant exchange of SDC coated SWCNT for pluronic coated SWCNT the suspension sat for 3 days, replacing stock of 1% pluronic each day. At the 3 day time-point the solution was centrifuged, absorbance measured and concentration of SWCNTs calculated as previously described[5]. Note that we anticipate there is exchange of SDC for pluronic, although it is possible that some pluronic overcoats the SDC. Because of the photophysical behavior of SWCNTs the use of a spectral shift in NIRF fluorescence to confirm surfactant exchange is not possible (was attempted). But what we do know, importantly, is that the dialyzed nanotubes are non-toxic (see cell studies and limited injury in vehicle only exposed mice) which support that the SDC does not become bioavailable. Furthermore, re-imaging of dialyzed SWCNT suspensions 3 months after preparations showed similar levels of fluorescence (Figure S2) suggesting the suspensions are stable.

To ensure biocompatibility, small airway epithelial cells (SAEC) were exposed to various doses of SWCNTs (0.2, 2.0, 20 and 50 ug/ml) for 24 hours and cell viability was determined using a standard trypan blue assay. This assay was used to avoid interference issues encountered for other more common assays (i.e. MTT) that utilize fluorescence or absorbance outputs. Exposure of cells to SDC alone caused 100% loss in viability. Average length of SWCNTs was estimated to be ~ 1.0 μm using standard TEM and AFM analysis (Figure 1).

2.2.   Animal Exposures

Animal care, exposures, and daily monitoring of health conditions were conducted using an approved IACUC protocol (#201408654) following university animal use and ethics policy. Two separate animal experiments were performed. The first was a smaller pilot study to optimize SWCNT recovery methods and NIRF imaging technology of lung tissues. C57BL/6 male mice (The Jackson Laboratory, Bar Harbor, ME) approximately 12 weeks of age, and commonly used for toxicity studies, were exposed to low, mid and high doses of dialyzed SWCNTs (10μg, 18μg, 26μg/mouse). These doses (mid and high) reflect the midrange of those administered to mice in the literature. The lower dose was chosen to assess the capability of NIRFI to capture quantities of SWCNTs in biological matrices at or below the dose of what other technologies (Raman) can assess. Mice were exposed to pluronic vehicle or SWCNTs by intratracheal (IT) instillation, a delivery method widely used by the pulmonary community which allowed us to have tight control of the dose delivered. For IT administration, mice were anesthetized with a cocktail of Ketamine and Xylazine at 100mg/kg and up to 5mg/kg body weight (Patterson Veterinaries Inc., Charlotte, NC) respectively, using intraperitoneal injection. Once anesthetized, the mouse was positioned on the rodent-tilting work station and inoculated with up to 40 μl of treatment sample at the entrance of the trachea. Mice received dialyzed SWCNTs (SG65i) or dialyzed pluronic (vehicle control), (N=6 for recovery at 18 μg/ml; N= 4 per group per dose for a total of 16 mice). Following intratracheal instillation, the mouse was placed on a heating pad, and monitored for recovery from anesthesia. Animals were kept in individually ventilated cages in a BSL2+ laboratory throughout the duration of the experiments. During the study period animals were monitored for distress at least once daily. A subset of animals (N=6, 18 μg dose) were immediately sacrificed and lungs used for determination of SWCNT recovery (see below). The remaining mice were sacrificed 7 days post exposure to assess SWCNT quantification using methods described below. All animals were sacrificed with an intraperitoneal injection of sodium pentobarbital at 100 mg/kg (Fatal Plus Solution, Patterson Veterinaries Inc., Charlotte, NC). All lungs were imaged immediately and excised (secondary method of euthanasia). Note the lack of background fluorescence observed in both whole lung tissues and histological section preparations which is an important advantage of this approach (Figure S3).

A second study was performed to track and quantify SWCNTs and determine the pulmonary response of SWCNTs exposed mice during a 21 day exposure. For this study C57BL/6 male mice approximately 12 weeks of age were exposed to a single bolus of SWCNTs (20 μg) by intratracheal instillation as described above (N=6 controls; N=10 SWCNT). , At sacrifice, lungs from all mice were imaged (N=6 controls and N=10 SWCNT exposed) and used for

semi-quantitative analysis. A subset of whole lungs (N=3 controls and N=6 treated) were homogenized and processed for SWCNT quantitation. Finally, the left lungs of remaining mice were processed for histopathological analysis (N=3 controls, N=4 exposed).

2.3. NIRF Imaging and Semi-quantification

At various time-points (7 days for study 1 and 3, 7, 14, 21 days for study 2) mice were euthanized with an intraperitoneal injection of sodium pentobarbital at 100mg/kg and the lungs were carefully excised, keeping the trachea attached. Excised lungs were weighed and imaged with NIRF as described previously with a few method modifications[5]. SWCNTs were excited with a Visotek 30 watt fiber coupled diode laser at 808 nm excitation wavelength (1, 5 and 3 watts output power, Visotek, Inc. Livonia, MI, USA). A 900 nm dichroic mirror (Thor Labs, Newton, NJ, USA) was used to reflect laser onto the sample. Fluorescence emission was then transmitted through the dichroic mirror, passed through two 1000 nm longpass filters (Thor Labs, Newton, NJ, USA), and finally imaged onto the detector by a 18–108 mm C mount zoom lens (Thor Labs, Newton, NJ, USA). Princeton Instruments OMA V InGaAs two dimensional array detector (320×256 pixels) was used to capture SWCNT emissions. The lower limit of quantitation of the SWCNTs in suspension was ~ 075 ng. WinView Software (Princeton Instruments, Trenton, NJ, USA) was used to record and save images. NIRF images collected for each sample were exported into Igor Pro 6.2 for semi-quantitative analysis based on a method previously reported[5]. Images were processed into x,y,z matrix waves and background subtraction was applied. Each sample was smoothed (Savitsky-Golay 3 point algorithm), and thresholded. Pixel intensity was integrated to give an averaged intensity multiplied by the area sampled (320×256 pixels), yielding a fluorescence intensity value for each SWCNT exposed lung. These intensity values were averaged by treatment group and plotted as integrated fluorescence intensity.

2.4. Quantification of SWCNTs in Lung Tissue

Prior to quantification of experimental samples, we determined the recovery of SWCNT in mouse lung tissues. For these experiments, 18 µg of SWCNT were instilled into the lungs of mice (N=6) and immediately collected, homogenized in SDC/proteinase K and analysed with NIRF spectral methods. The concentration of SWCNTs obtained was calculated for each sample based on the spectral peaks and compared to the starting concentrations. This value was converted to a percent of the total original 18 µg of SWCNTs. The average recovery was 66% +/− 0.06 µg.

Knowing the recovery, we then quantified SWCNT lung burdens at varied doses (low, med, high) after 7 days in a preliminary experiment and then for a more extensive timecourse (up to 21 days for 1 dose of 20 µg) in a second experiment. Lung samples were homogenized in 2mL 2% sodium deoxycholate using a 1/8" microtip probe sonicator (Branson Sonifier) at 50% amplitude for 10 minutes on ice. After sonication, 2mL of proteinase K and buffer was added to each sample (80µL proteinase K (20ul PK /ml, 720µL ATL buffer and 1200µL water) and incubated for 24h at 60°C. Upon completion of incubation, NIRF spectra were collected using NS1 spectrofluorometer (Applied NanoFluorescence, Houston, TX) at three laser excitation wavelengths (638, 691, and 782 nm) and the concentration of SWCNT was calculated based on a standard curve.

2.5. Pathology Evaluation and Localization of SWCNTs

Pathology evaluation of lung tissue on histological sections was carried out by a board-certified veterinary pathologist (Dr. William Castleman) for the second 21 day study only. To prepare the tissues the left lungs of five mice per treatment group were instilled with 4 % paraformaldehyde in PBS (pH 7.3) *in situ* using a 1-ml syringe. Lungs were excised, fixed in 4 % paraformaldehyde, and embedded in a paraffin block. Lungs, bisected in the sagittal plane, were then dehydrated through alcohol series, cleared in xylene and embedded in paraffin. Paraffin sections were stained with hematoxylin and eosin for histopathologic and morphometric analysis[13]. H & E prepared histological sections were then examined with a Nikon Eclipse Ti-U light microscope attached to our NIRFI detector for further localization of SWCNTs at each time-point.

2.6. Statistical Analysis

SPSS version 20 (IBM, Chicago, IL) software for Windows was used to carry out all statistical analysis. The dataset was tested for normality and a one-way ANOVA with Dunett's test were used for multiple comparison analysis between treatment groups. The null hypothesis was rejected at a p-value < 0.05.

3.0. Results and Discussion

3.1. Characterization and Optimization of NIRF Imaging

We employed pristine SWCNTs that are possess unique properties over other types of CNTs in that they are innately fluorescent and have been previously described and heavily characterized by our group[5]. A representative TEM image (before and after suspension), chirality plot, diameter distribution and AFM images are shown in Figure 1. Both TEM and AFM images were used to estimate the length (> 500 nm) of suspended SWCNTs and also show enhanced dispersion of the tubes in the presence of pluronic . Importantly, these particular SWCNTs allow for detection by fluorescence without covalent modification or alteration of the nanotubes. Optimal fluorescence of the SWCNTs however is only achieved in dispersants (e.g. sodium deoxycholate, sodium dodecyl sulfate) that are typically not biocompatible and therefore an inherent challenge is to preserve their innate fluorescence properties under biocompatible conditions. This is demonstrated where the fluorescence signal emitted from SWCNTs suspended in biocompatible pluronic is reduced compared to the non-biocompatible but highly dispersible sodium deoxycholate (SDC) (Figure 2A–B). These results clearly demonstrate the quenching of NIRF signal that occurs in pluronic compared to SDC. After further dialyzing SDC-suspended SWCNTs in pluronic using a surfactant-exchange method adapted from Welsher et al., 2009 we were able to maintain fluorescence properties by improving the quantum yield similar to SWCNTs suspended in SDC but with no measurable cytotoxicity (Figure 2C)[4, 9].

SDC is a good dispersant, but is known to be toxic to biological systems. To ensure that our dialyzed SWCNTs were biocompatible, we exposed small airway epithelial cells (SAEC) to various doses of dialyzed SWCNTs and quantified cell viability. Results of these experiments show no measurable toxicity while SDC caused 100% cytotoxicity. Toxicity (measured by the same method) of pluronic coated only SWCNTs has been previously

published by our group which also show no toxicity[7, 9]. These results support that there was maximal exchange of pluronic for SDS or that the pluronic effectively overcoats the SDC. Since the dialyzed SWCNTs remained in the media for 24 hours, if SDS were to leach off the nanotubes, we would have expected to see toxicity. It is also worth mentioning that fluorescence was still detectable from a working stock of dialyzed SWCNTs up to 3 months after preparation, suggesting that the SDC does not leach from the SWCNTs (Figure S2).

3.2.   Quantification of SWCNTs in mouse lung tissues

A series of experiments were then performed to optimize SWCNT quantification in lung tissue homogenates using NIRF spectrometry. For these experiments dialyzed SWCNTs were instilled intratracheally into mice at three doses (10 μg, 18 μg, or 26 μg/mouse). This is a very well-accepted method of delivery when inhalation is not an option and it afforded us tight control of the dose delivered. We employed doses within the range of workplace exposure assessment and thus representative of human occupational exposure[14]. These doses are also consistent with our previous studies with SWCNTs and also with studies that have utilized this effective dose where inhalation was employed as an exposure route for 7–8 days in mice[15–16]. Lung tissues were extracted, homogenized in SDC and NIRF emission spectra was used to quantify recovery which averaged 66.1%. NIRF images were also collected on whole lungs and SWCNTs were semi-quantified based on the method described below.

We then demonstrated the utility of our methods to track and quantify SWCNTs in lung tissues and addressed questions related to pulmonary retention and distribution by exposing mice to a single dose (20 μg/mouse) of dialyzed SWCNTs. Observations were conducted during five time-points over the 21 day exposure window (0, 3, 7, 14, and 21 days). At each time point, excised lung tissues were imaged and SWCNTs quantified using NIRFI and spectroscopic methods (Figure 3). Each time-point included a SWCNT exposure group and a dialyzed pluronic exposure group (vehicle control). Strong SWCNT-derived fluorescence was consistently detected over the 21 day time course using NIRFI and semi-quantitation (based on total raw pixel intensities) of these images was consistent with SWCNT burdens measured by NIRF spectroscopy in whole lung tissue homogenates. For instance, less SWCNT-derived fluorescence observed by imaging was consistent with fewer μg of SWCNTs calculated in homogenized tissue samples using spectral analysis. Average quantities of SWCNTs in lung tissues from each exposure group were determined and the spectroscopic and NIRFI methods were compared (Figure 4). In general, both methods show a comparable decreasing trend in SWCNT average fluorescence intensity and mass (μg / mouse) recovered over the 21 day exposure period although this trend was not statistically significant. Perhaps this steady decrease in SWCNTs is a result of early action of mucociliary clearance that is likely to occur in the upper airways. In a study by Shinohara et al.,[17] approximately 30% of administered MWCNTs were suggested to be cleared by bronchial ciliary motion within 24 h of administration, but then remained stable over time for up to 364 days after instillation, suggesting that MWCNTs were not readily cleared. It is possible that a similar mechanism accounts for the initial drop in SWCNT concentration by day 3. It is also possible that some level of biotransformation contributes to loss of signal however, it is important to note that this particular type of CNT (pristine SWCNT) are minimal degraded by enzymes compared to those that are surface functionalized (i.e.

hydroxylated) and degraded much more efficiently[18]. Further experiments with shorter and longer timepoints would help to answer such questions in future studies.

3.3. SWCNT localization and lung injury following exposure

NIRF imaging of histological lung tissue sections also displayed persistence of SWCNTs over the exposure timeframe and allowed for localization in regions of the lung cells and tissue. Using brightfield microscopy, initial deposition of nanotubes predominantly in terminal bronchiole alveolar duct (TBAD) junctions and proximal acinar areas were noted on the day of exposure (day 0) that induced peak inflammatory reactions characterized by macrophages and neutrophils by 3 to 7 days after exposure (Figure 5), consistent with our previous report[7]. We also observed associated hyperplasia of type II alveolar epithelial cells and bronchiolar epithelial cells with alveolar wall disruption. By 14 to 21 days after inoculation, inflammatory reactions dominated by macrophages with nanotube aggregates were concentrated at TBAD regions. Using the NIRF imaging technique directly on tissue sections, nanotube aggregation was observed to be associated with mild to severe remodeling of alveolar and bronchiolar walls in TBAD and proximal acinar areas. Airway remodeling was characterized by alveolar and bronchiolar wall thickening with fibroblast proliferation and fibrosis as well as by ongoing hyperplasia of bronchiolar and alveolar type II epithelial cells. SWCNT distributions are shown in Figure 6 using NIRFI and were consistent with inflammatory responses and dominated by macrophage and neutrophil populations, as reported earlier in the pathology findings, shown in Figure 5.

The biopersistence and inflammatory responses observed in this study are consistent with the growing body of literature on SWCNT fate and effects in the lung[2, 10, 19–20] including alveolar wall restructuring, granuloma formation as early as day 7 post initial exposure, and fibrosis in a time and dose dependent manner[10, 20–23]. Such injury is consistent with the nanotubes themselves and is not likely the result of metal toxicity – although the metals may contribute to a small amount of oxidative stress. In our particular study, the content of cobalt and molybdenum in 'as prepared' SWCNT suspensions are low (< 4 % (w/w)) and only a small fraction (<3%) leaches. Therefore, we anticipate that metal contamination contributes minimally, at best, to any biological effects (fibrosis).

SWCNTs have been documented in alveolar spaces up to 1 year post exposure with early onset of macrophage recruitment detected as early as 24 hours post exposure, although quantitation of nanotubes was not performed[22, 24]. While the toxicity literature regarding the molecular and cellular response of the lung to CNTs is robust, characterization of clearance/ retention using quantitative approaches has been limited thus far. Yet, studies of lung clearance/retention are essential for understanding the potential for adverse health effects of SWCNT. Although we did not perform inhalation studies, we anticipate that our NIRF system and methods would work well for such exposures as the SWCNTs fluoresce well both in dry and suspended form (pluronic/SDC/gum arabic).

3.4. Advantages and limitations of NIRF for toxicity assessments

As with most techniques there are some limitations. One limitation of utilizing NIRF in this capacity is that it cannot be applied to all types of CNTs as they do not possess intrinsic NIR

fluorescence properties Second, the potential for decreases in NIRF emission under aggregation conditions can be difficult to precisely control. It is important to note, however, that NIRF emission from SWCNTs in our samples is a strong indication that nanotubes in our suspensions and samples were individually solubilized through the dispersion treatment with surfactants. To ensure that decreases in NIRF signals were indicative of clearance we also homogenized samples and dispersed the remaining SWCNTs in SDC. This would account for any "bundled" SWCNT within the tissues that might have been essentially invisible to the NIRF imaging system (i.e. the SWCNT would have been exfoliated and dispersed by the SDC solution, rendering them NIRF active again). In addition, the results of these analyses matched well with the results from the images.

There are several advantages that NIRF affords compared to other techniques such as the rapid output of biodistribution information in real-time at both the whole tissue and histological level with low background fluorescence (Figure S2). Our study also demonstrates the ability to track and quantify these nanotubes without the requirement for labeling or tagging, therefore maintaining the veracity of their physicochemical properties and behavior *in vivo*. It is also worth noting that a common approach to determining CNT lung burdens is to homogenize whole lungs and quantify relevant metals. This method likely provides a good estimate however, it is still not clear that all metals stay complexed with the nanotubes in vivo. Because our method quantifies the CNTs we do not have to consider how the metals behave. Finally, our NIRF method has the ability to localize SWCNTs with ease without extensive scanning and on the same sections utilized for histopathological analysis, revealing SWCNTs in areas where larger aggregates are not apparent and without extensive scanning. While certain applications such as Raman spectroscopy also has these advantages NIRF does offer additional and substantial benefits. In particular, NIR has an order of magnitude higher sensitivity than Raman in biological tissues[25]. Hong et al.[26], also explained in a review paper that inherently weak magnitude of the Raman effect limits its sensitivity which can hamper its use in biomedical applications and may account for why studies that use Raman tend to administer higher doses (e.g. 40 μg – 1.0 mg per mouse)[27]. In addition, Raman signal of SWCNTs may also damage tissues and distort signals if the intensity of the laser is too strong[26] and background signals from endogenous Raman scattering can be an issue[28]. In another study where Raman was used to map biodistribution of CNTs in blood and lungs of rodents, the authors discuss the difficulty of CNT detection due to large between animals making it difficult to quantify the amount of nanotubes present, and observation likely due to low sensitivity[29]. This is not to say techniques like Raman are less superior to NIRF but wwe do recommend however, that both imaging and spectroscopic quantitation methods complement each other and can be utilized to provide additional evidence of SWCNT biodistribution and collectively offer important information to the field of nanomaterial toxicology and health and safety.

Supplementary Material

Refer to Web version on PubMed Central for supplementary material.

Acknowledgements

List of Abbreviations

BALF	Bronchoalveolar lavage fluid
DLS	Dynamic light scattering
TEM	Transmission electron microscopy
HDR	Hydrodynamic radius
ICP-MS	Induction coupled mass spectrometry
NM	Nanomaterial
qPCR	Quantitative real-time polymerase chain reaction
SWCNT	single-walled carbon nanotube
SDC	sodium deoxycholate
TBAD	terminal bronchiole alveolar duct

References

1. Donaldson K; Murphy FA; Duffin R; Poland CA, Asbestos, carbon nanotubes and the pleural mesothelium: a review of the hypothesis regarding the role of long fibre retention in the parietal pleura, inflammation and mesothelioma. Part Fibre Toxicol 2010, 7, 5. [PubMed: 20307263]

2. Mercer RR; Scabilloni JF; Hubbs AF; Battelli LA; McKinney W; Friend S; Wolfarth MG; Andrew M; Castranova V; Porter DW, Distribution and fibrotic response following inhalation exposure to multi-walled carbon nanotubes. Part Fibre Toxicol 2013, 10, 33. [PubMed: 23895460]

3. Sadik OA; Zhou AL; Kikandi S; Du N; Wang Q; Varner K, Sensors as tools for quantitation, nanotoxicity and nanomonitoring assessment of engineered nanomaterials. J Environ Monit 2009, 11 (10), 1782–800. [PubMed: 19809701]

4. Welsher K; Liu Z; Sherlock SP; Robinson JT; Chen Z; Daranciang D; Dai H, A route to brightly fluorescent carbon nanotubes for near-infrared imaging in mice. Nat Nanotechnol 2009, 4 (11), 773–80. [PubMed: 19893526]

5. Bisesi JH Jr.; Merten J; Liu K; Parks AN; Afrooz AR; Glenn JB; Klaine SJ; Kane AS; Saleh NB; Ferguson PL; Sabo-Attwood T, Tracking and quantification of single-walled carbon nanotubes in fish using near infrared fluorescence. Environ Sci Technol 2014, 48 (3), 1973–83. [PubMed: 24383993]

6. Khan IA; Aich N; Afrooz AR; Flora JR; Schierz PA; Ferguson PL; Sabo-Attwood T; Saleh NB, Fractal structures of single-walled carbon nanotubes in biologically relevant conditions: role of chirality vs. media conditions. Chemosphere 2013, 93 (9), 1997–2003. [PubMed: 23920360]

7. Chen H; Zheng X; Nicholas J; Humes ST; Loeb JC; Robinson SE; Bisesi JH Jr.; Das D; Saleh NB; Castleman WL; Lednicky JA; Sabo-Attwood T, Single-walled carbon nanotubes modulate pulmonary immune responses and increase pandemic influenza a virus titers in mice. Virol J 2017, 14 (1), 242. [PubMed: 29273069]

8. Bardi G; Vittorio O; Maffei M; Pizzorusso T; Costa M, Adipocytes differentiation in the presence of Pluronic F127-coated carbon nanotubes. Nanomed-Nanotechnol 2009, 5 (4), 378–381.

9. Sanpui P; Zheng X; Loeb JC; Bisesi JH Jr.; Khan IA; Afrooz AR; Liu K; Badireddy AR; Wiesner MR; Ferguson PL; Saleh NB; Lednicky JA; Sabo-Attwood T, Single-walled carbon nanotubes

increase pandemic influenza A H1N1 virus infectivity of lung epithelial cells. Part Fibre Toxicol 2014, 11, 66. [PubMed: 25497303]

10. Wang L; Castranova V; Mishra A; Chen B; Mercer RR; Schwegler-Berry D; Rojanasakul Y, Dispersion of single-walled carbon nanotubes by a natural lung surfactant for pulmonary in vitro and in vivo toxicity studies. Part Fibre Toxicol 2010, 7, 31. [PubMed: 20958985]

11. Wang X; Duch MC; Mansukhani N; Ji ZX; Liao YP; Wang MY; Zhang HY; Sun BB; Chang CH; Li RB; Lin SJ; Meng H; Xia T; Hersam MC; Nel AE, Use of a Pro-Fibrogenic Mechanism-Based Predictive Toxicological Approach for Tiered Testing and Decision Analysis of Carbonaceous Nanomaterials. Acs Nano 2015, 9 (3), 3032–3043. [PubMed: 25646681]

12. Khan IA; Afrooz AR; Flora JR; Schierz PA; Ferguson PL; Sabo-Attwood T; Saleh NB, Chirality affects aggregation kinetics of single-walled carbon nanotubes. Environ Sci Technol 2013, 47 (4), 1844–52. [PubMed: 23343128]

13. Li X; Castleman WL, Effects of 4-ipomeanol on bovine parainfluenza type 3 virus-induced pneumonia in calves. Vet Pathol 1991, 28 (5), 428–37. [PubMed: 1661042]

14. Erdely A; Dahm M; Chen BT; Zeidler-Erdely PC; Fernback JE; Birch ME; Evans DE; Kashon ML; Deddens JA; Hulderman T; Bilgesu SA; Battelli L; Schwegler-Berry D; Leonard HD; McKinney W; Frazer DG; Antonini JM; Porter DW; Castranova V; Schubauer-Berigan MK, Carbon nanotube dosimetry: from workplace exposure assessment to inhalation toxicology. Part Fibre Toxicol 2013, 10 (1), 53. [PubMed: 24144386]

15. Porter DW; Hubbs AF; Chen BT; McKinney W; Mercer RR; Wolfarth MG; Battelli L; Wu N; Sriram K; Leonard S; Andrew M; Willard P; Tsuruoka S; Endo M; Tsukada T; Munekane F; Frazer DG; Castranova V, Acute pulmonary dose-responses to inhaled multi-walled carbon nanotubes. Nanotoxicology 2013, 7 (7), 1179–94. [PubMed: 22881873]

16. Sargent LM; Porter DW; Staska LM; Hubbs AF; Lowry DT; Battelli L; Siegrist KJ; Kashon ML; Mercer RR; Bauer AK; Chen BT; Salisbury JL; Frazer D; McKinney W; Andrew M; Tsuruoka S; Endo M; Fluharty KL; Castranova V; Reynolds SH, Promotion of lung adenocarcinoma following inhalation exposure to multi-walled carbon nanotubes. Part Fibre Toxicol 2014, 11, 3. [PubMed: 24405760]

17. Shinohara N; Nakazato T; Ohkawa K; Tamura M; Kobayashi N; Morimoto Y; Oyabu T; Myojo T; Shimada M; Yamamoto K; Tao H; Ema M; Naya M; Nakanishi J, Long-term retention of pristine multi-walled carbon nanotubes in rat lungs after intratracheal instillation. J Appl Toxicol 2016, 36 (4), 501–9. [PubMed: 26712168]

18. Hou J; Wan B; Yang Y; Ren XM; Guo LH; Liu JF, Biodegradation of Single-Walled Carbon Nanotubes in Macrophages through Respiratory Burst Modulation. Int J Mol Sci 2016, 17 (3).

19. Shvedova AA; Kisin E; Murray AR; Johnson VJ; Gorelik O; Arepalli S; Hubbs AF; Mercer RR; Keohavong P; Sussman N; Jin J; Yin J; Stone S; Chen BT; Deye G; Maynard A; Castranova V; Baron PA; Kagan VE, Inhalation vs. aspiration of single-walled carbon nanotubes in C57BL/6 mice: inflammation, fibrosis, oxidative stress, and mutagenesis. Am J Physiol Lung Cell Mol Physiol 2008, 295 (4), L552–65. [PubMed: 18658273]

20. Shvedova AA; Kisin ER; Murray AR; Mouithys-Mickalad A; Stadler K; Mason RP; Kadiiska M, ESR evidence for in vivo formation of free radicals in tissue of mice exposed to single-walled carbon nanotubes. Free Radic Biol Med 2014, 73, 154–65. [PubMed: 24863695]

21. Kagan VE; Konduru NV; Feng W; Allen BL; Conroy J; Volkov Y; Vlasova II; Belikova NA; Yanamala N; Kapralov A; Tyurina YY; Shi J; Kisin ER; Murray AR; Franks J; Stolz D; Gou P; Klein-Seetharaman J; Fadeel B; Star A; Shvedova AA, Carbon nanotubes degraded by neutrophil myeloperoxidase induce less pulmonary inflammation. Nat Nanotechnol 2010, 5 (5), 354–9. [PubMed: 20364135]

22. Shvedova AA; Yanamala N; Kisin ER; Tkach AV; Murray AR; Hubbs A; Chirila MM; Keohavong P; Sycheva LP; Kagan VE; Castranova V, Long-term effects of carbon containing engineered nanomaterials and asbestos in the lung: one year postexposure comparisons. Am J Physiol Lung Cell Mol Physiol 2014, 306 (2), L170–82. [PubMed: 24213921]

23. Di YP; Tkach AV; Yanamala N; Stanley S; Gao S; Shurin MR; Kisin ER; Kagan VE; Shvedova A, Dual acute proinflammatory and antifibrotic pulmonary effects of short palate, lung, and nasal epithelium clone-1 after exposure to carbon nanotubes. Am J Respir Cell Mol Biol 2013, 49 (5), 759–67. [PubMed: 23721177]

24. Jacobsen NR; Moller P; Jensen KA; Vogel U; Ladefoged O; Loft S; Wallin H, Lung inflammation and genotoxicity following pulmonary exposure to nanoparticles in ApoE−/−mice. Part Fibre Toxicol 2009, 6, 2. [PubMed: 19138394]

25. Petersen EJ; Flores-Cervantes DX; Bucheli TD; Elliott LC; Fagan JA; Gogos A; Hanna S; Kagi R; Mansfield E; Bustos AR; Plata DL; Reipa V; Westerhoff P; Winchester MR, Quantification of Carbon Nanotubes in Environmental Matrices: Current Capabilities, Case Studies, and Future Prospects. Environ Sci Technol 2016, 50 (9), 4587–605. [PubMed: 27050152]

26. Hong H; Gao T; Cai W, Molecular Imaging with Single-Walled Carbon Nanotubes. Nano today 2009, 4 (3), 252–261. [PubMed: 21754949]

27. Yang ST; Wang X; Jia G; Gu Y; Wang T; Nie H; Ge C; Wang H; Liu Y, Long-term accumulation and low toxicity of single-walled carbon nanotubes in intravenously exposed mice. Toxicology letters 2008, 181 (3), 182–9. [PubMed: 18760340]

28. Cherukuri P; Bachilo SM; Litovsky SH; Weisman RB, Near-infrared fluorescence microscopy of single-walled carbon nanotubes in phagocytic cells. J Am Chem Soc 2004, 126 (48), 15638–9. [PubMed: 15571374]

29. Ingle T; Dervishi E; Biris AR; Mustafa T; Buchanan RA; Biris AS, Raman spectroscopy analysis and mapping the biodistribution of inhaled carbon nanotubes in the lungs and blood of mice. Journal of applied toxicology : JAT 2013, 33 (10), 1044–52. [PubMed: 23047664]

Highlights

- Near-infrared fluorescence (NIRF) can be utilized to track and quantify SWCNTs in tissues in vivo

- Critical information on clearance of SWCNTs from the lung

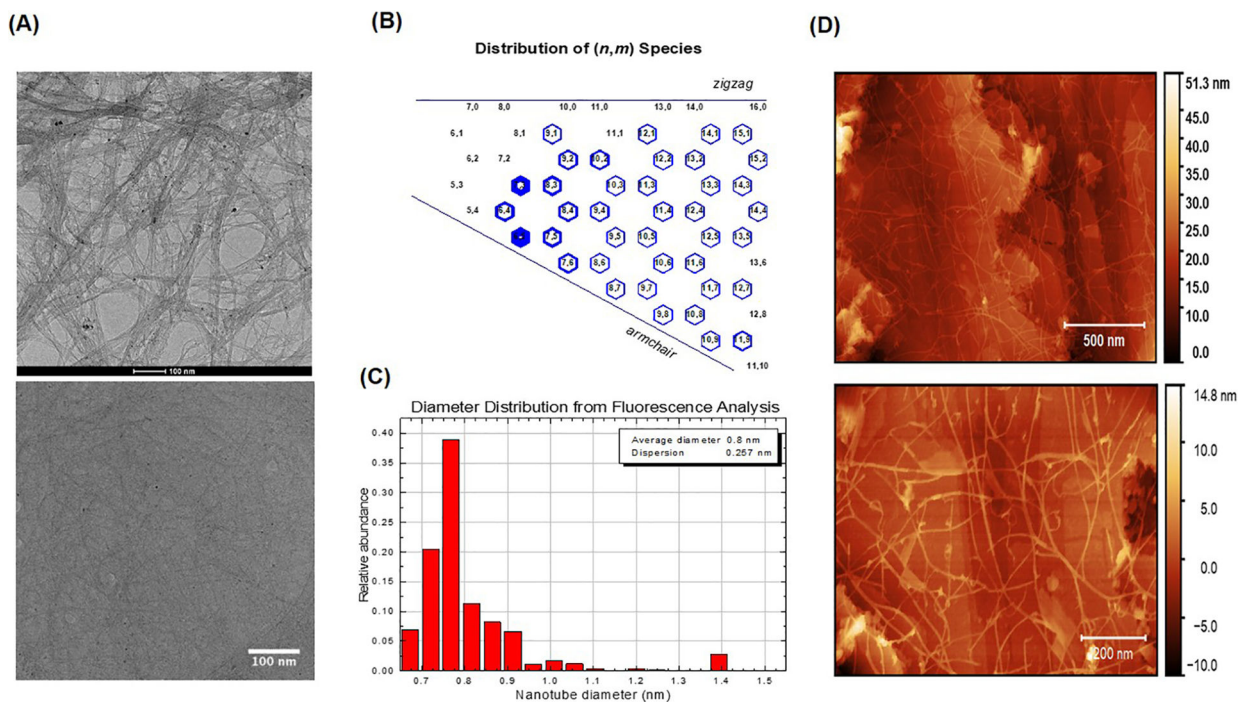- Can be performed in tandem with toxicological health assessments

Figure 1.

Unique properties and characterization of SG65 SWCNTs by (A) TEM images of SWCNT as purchased (Top) and working stock dialyzed in pluronic /SDC (bottom); (B) Chirality plot; (C) Diameter distribution, and (D) AFM images of SWCNT as purchased (Top) and working stock dialyzed in pluronic /SDC (bottom).
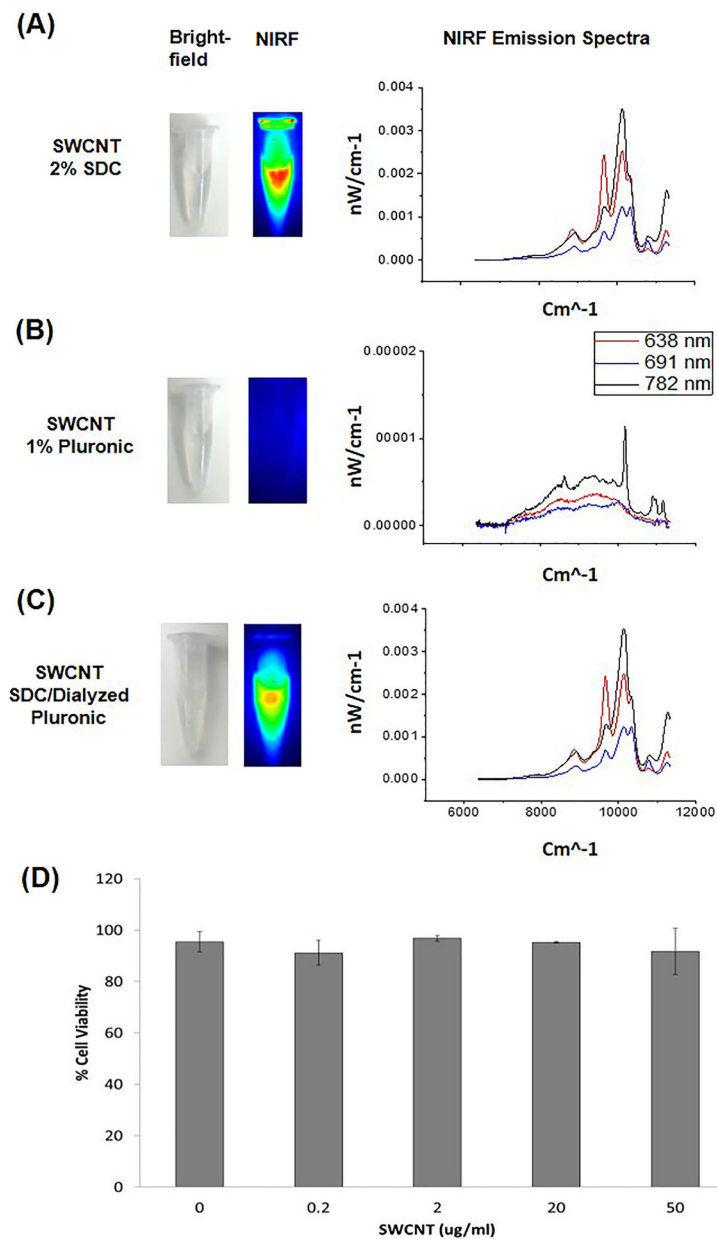
Figure 2.
NIR imaging of SWCNT suspensions (left) and corresponding spectra (right). (A) SWCNTS prepared in 2% SDC, (B) 1% pluronic and (C) dialyzed puronic/SDC. Note the differences in intensity and spectral profiles for SWCNTs that are less bundled (2% SDC and dialyzed) and loss of fluorescence with pluronic only. To ensure dialyzed SWCNTs did not elicit toxicity, small airway epithelia cells were exposed to a range of concentrations (μg/ml) for 24 hours and viability quantified. No toxicity was observed at any of the doses tested (N=3).
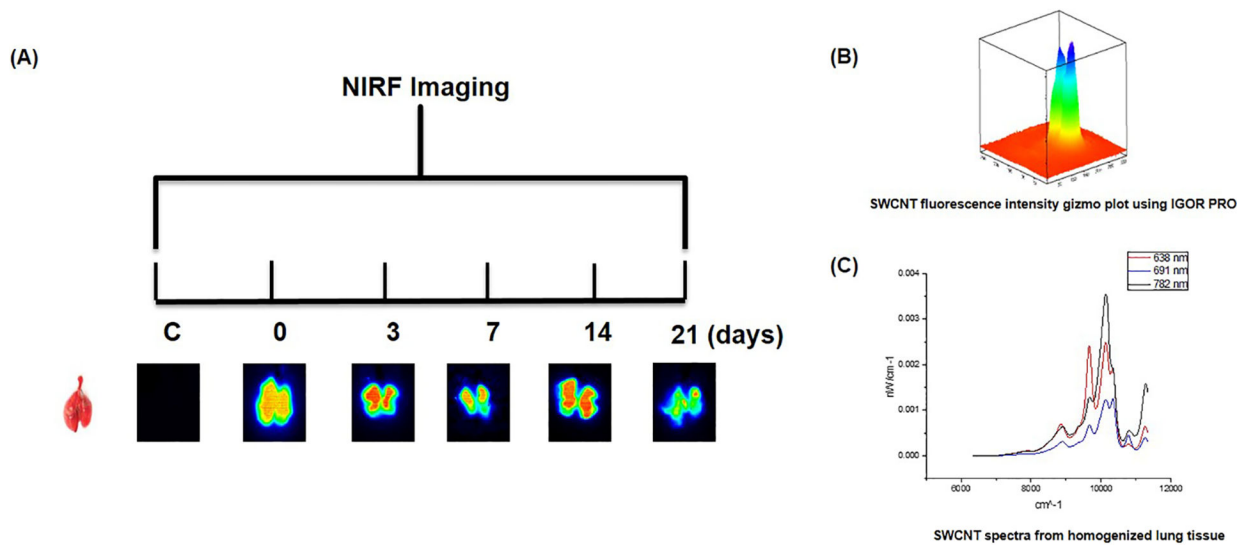
Figure 3.
(A) Timeline of near-infrared fluorescence images and bright field images of control and SWCNT-exposed lungs captured over the 21-day exposure period. (B) Example SWCNT pixel intensity plot used to quantify images. (C) Example NIRF spectra from homogenized tissue sample used to quantify SWCNTs
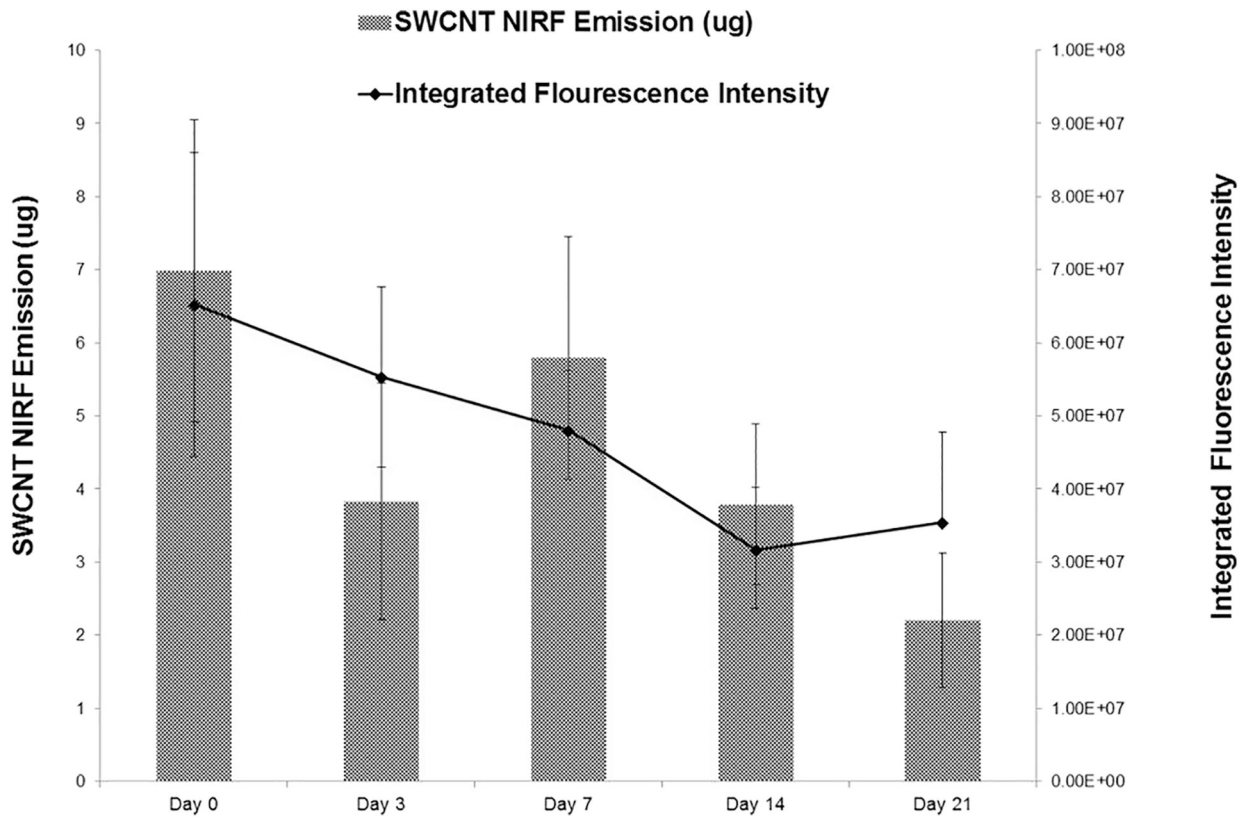
Figure 4.
Quantification of SWCNTs present in lung tissue from exposed mice using NIRF
spectroscopy (bars) and NIRF images (line). Graph of SWCNT mass (µg) recovered from
lung tissue across treatment groups versus fluorescence recovery of SWCNT exposed lungs
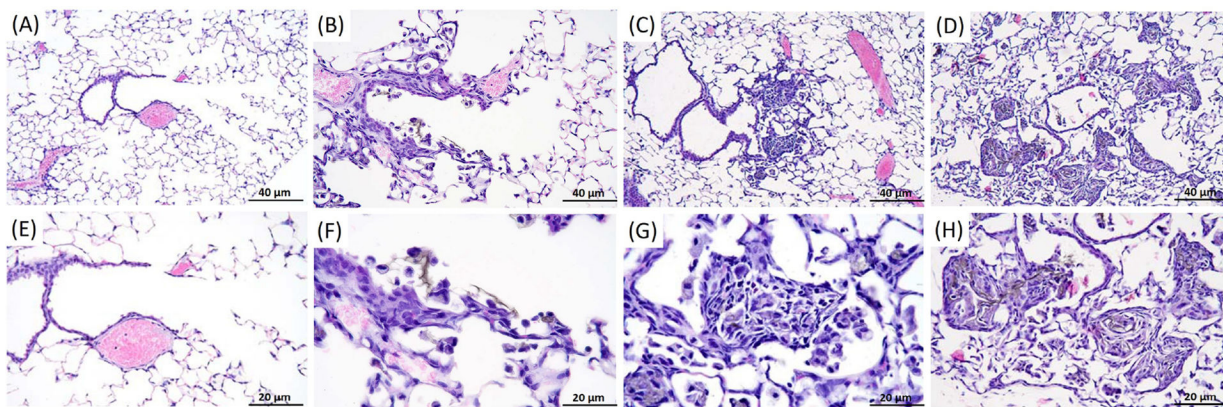was measured over the 21-day exposure period (N=6).

Figure 5.
(A) Histopathology images of lung tissue sections from a representative control mouse and mouse exposed to SWCNT for 0 (A,E) 3 (B.F), 7 (C,G), and 21 (D,H) days. Lung tissues sections were stained with H&E and images captured using light microscopy. Increased magnification of lung tissue sections are shown in E-H (scale bar 20 μm of the images above, A-D (scale bar 40 μm). Pictures represent consistent observations from N=4 mice per treatment group.
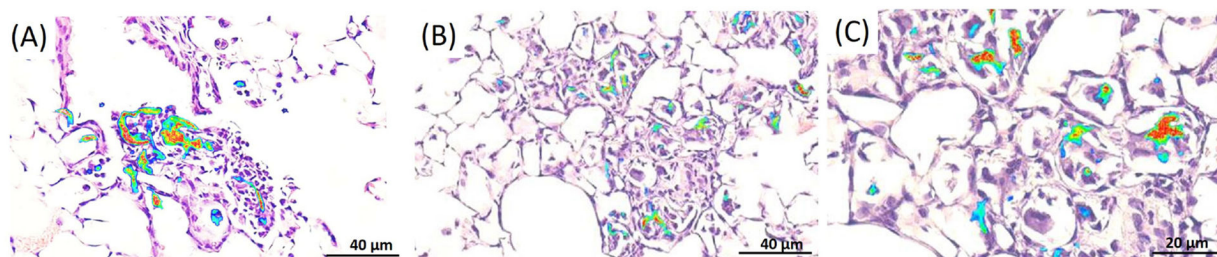
Figure 6.
Lung tissue sections overlaid with NIRF imaging showing the distribution of SWCNT at 3 days (A) and 21 days (B,C). Pictures represent consistent observations from N=4 mice per treatment group. Note the presence of SWCNTs in areas where 'black aggregates' were not visible by brightfield microscopy.